LIGHT SCATTERING INVESTIGATION OF BLACK TURMERIC (CURCUMA CAESIA): A COMPARATIVE STUDY WITH ESTABLISHED MIE THEORY

Farhana Hussain[1] and Sanchita Roy[1*]

[1]*Department of Physics, School of Applied Sciences, University of Science and Technology, Meghalaya, District- Ri Bhoi, 793101, Meghalaya, India.*

[*]Corresponding Author: rsanchita1@gmail.com

(Received 25 September 2025; revised 22 November 2025; accepted 22 November 2025; published 6 April 2026)

Abstract: This study reports measurements of the angular distribution of the scattering matrix elements d_{11} and d_{12} for randomly oriented sub-micron Black turmeric (Curcuma caesia) particles using a light scattering technique with a He–Ne laser at 632.8 nm. The volume scattering function and depolarization effects were experimentally investigated at room temperature (25°C). Theoretical predictions of d_{11} and d_{12} were obtained using Philip Laven's software, based on Mie theory, which describes light scattering by spherical or randomly oriented non-spherical particles. A significant deviation was observed between experimental results and theoretical profiles, indicating the strong influence of particle size, shape, and their distributions on scattering behavior. Given the organic nature of Black Turmeric, external factors such as temperature, humidity, and moisture can further alter scattering characteristics. While experiments can be extended to different temperatures, theoretical modeling remains restricted, as widely used light scattering codes do not account for temperature effects or distributions in size and shape. These findings highlight both the practical importance of experimental investigation for organic samples and the limitations of Mie theory in fully capturing the scattering behavior of Black Turmeric particles under varying conditions.

Keywords: Light scattering; Mie theory; Volume scattering function; Depolarization; Black Turmeric

PACS: 07.05.-t; 85.60.-q

1 Introduction

Among the many ways light interacts with matter, scattering stands out as a phenomenon that shapes both the subtle hues of the natural world and the intricate visual signatures of living systems. Emerging wherever electromagnetic waves encounter structural irregularities, it serves as a window into the morphology and optical nature of particles [1–3]. The interaction of light with matter not only enriches our understanding of fundamental physics but also drives innovation across diverse domains such as Biomedical Imaging, Material Characterization, Atmospheric Science, Optical Biosensing and Point-of-Care Diagnostics, Drug Delivery and Nanomedicine, Food and Agricultural Sciences, Environmental Monitoring and Remote Sensing, Nanotechnology etc. Light scattering, although conceptually simple, is governed by complex parameters including particle size, morphology, chemical composition, and refractive index [3, 4]. Upon striking a particle, photons may undergo absorption, refraction, or directional redistribution, generating scattering profiles that carry distinct imprints of the material's structural properties [5–8].

Among various theoretical approaches, Mie theory provides a rigorous solution for the scattering of electromagnetic waves by homogeneous, isotropic spherical particles and randomly oriented non-spherical particles [9, 10]. While widely used due to its analytical nature and broad applicability, Mie theory assumes idealized conditions that may not accurately represent the complexities of real-world samples, especially those with irregular

geometries or heterogeneous compositions [9–11]. Mie theory offers an accessible way to explore theoretical scattering behavior under controlled parameters, making it valuable for comparison with experimental results. It enables users to calculate and visualize various scattering parameters, including intensity patterns, polarization effects, and angular distributions etc [12, 13]. Mie Plot supports a wide range of input parameters such as particle size, refractive index, angular resolution, and wavelength, allowing for detailed and customizable simulations [11–13]. However, most widely used light scattering software lacks the capability to incorporate parameters such as size distribution, shape distribution, temperature, and other environmental factors [14, 15]. Its intuitive interface and flexible simulation options make it particularly useful for modeling how light interacts with spherical particles [16, 17].

In recent years, bio-organic materials have attracted growing interest due to their distinctive structural and optical properties. One such material, Black Turmeric (BT), contained sub-micron-sized particles and showed promising potential in fields such as medicine, cosmetics, and material science [18–20]. However, despite its relevance, minimal research was carried out to understand how this material scatters light, especially under well-controlled experimental conditions.

In this study, we examined the angular distribution of the scattering matrix elements d_{11} and d_{12} for randomly oriented sub-micron BT particles. We used a He-Ne laser with a wavelength of 632.8 nm to measure the volume scattering function, $\beta(\theta)$, and analyzed depolarization effects through the degree of linear polarization, $P(\theta)$, at room temperature [20–22]. In light scattering, $\beta(\theta)$ represents the volume scattering function, quantifying the scattered light intensity at angle θ, while $P(\theta)$ accounts for the degree of polarization change as light is scattered at angle θ.

`MiePlot` simulations provided valuable insights and served as baseline predictions, notable deviations emerged when compared to the measured scattering behavior of sub-micron BT particles. These differences underscore the limitations of Mie theory, especially when applied to complex biological samples with irregular shapes, internal inhomogeneities, and a range of particle sizes, conditions that deviate from the ideal assumptions of the model.

In this study, we investigated the angular distribution of scattering matrix elements d_{11} and d_{12} for sub-micron BT particles using a He-Ne laser at 632.8 nm. Experimental measurements of the $\beta(\theta)$ and $P(\theta)$ at room temperature were compared with theoretical predictions generated using Philip Laven's Mie Plot software. While Mie theory provided useful insights, significant discrepancies highlighted its limitations in modeling complex, irregular biological particles.

2 Methodological details

2.1 Scanning Electron Microscopy (SEM) of BT

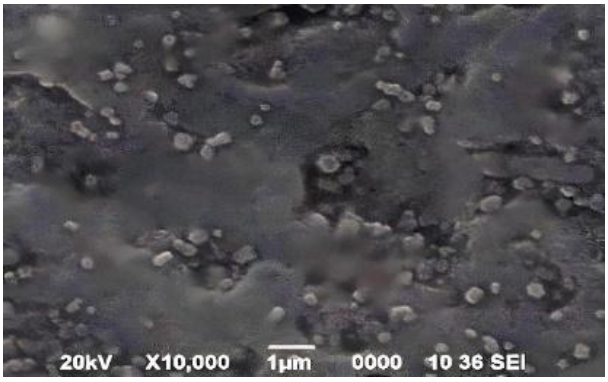

Figure 1: SEM image of BT

SEM images provided high-resolution insights into the morphology of the BT sample. The BT particles were observed to be nearly spherical, with a modal radius of approximately $0.25\mu m$ [14, 20]. The SEM image enabled us to find the parameters required to generate the theoretical scattering profile Mieplot. Accurate knowledge of particle size and shape is crucial for light scattering studies, as these parameters directly influence the scattering behavior. It is supported by Laven's software, though with limitations in parameters such as temperature, size distributions, and shape distributions, and the imaginary component of the refractive index.

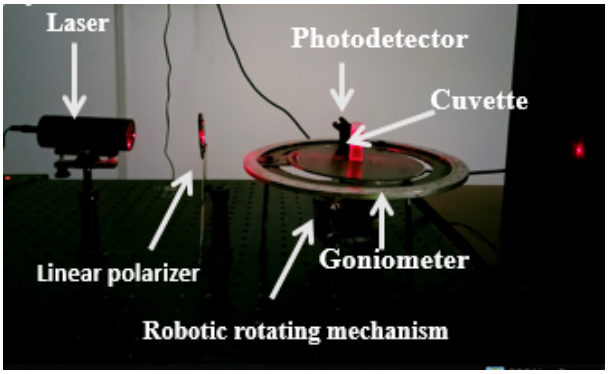

Figure 2: Laboratory-based static light scattering setup

2.2 Experimental Light Scattering Analysis

During the light scattering experiments, the detector was first placed at 0° and then rotated in 1° increments from 10° to 170° to measure the angular distribution of the scattered light. Fig. 2 shows the laboratory-based light scattering setup used for the experimentation and analysis. The intensity of the scattered light, corresponding to the d_{11} and d_{12} elements of the Mueller matrix, was recorded using the light scattering setup. These measurements were then used to calculate the $\beta(\theta)$ and $P(\theta)$. For ease of comparison, the resulting $\beta(\theta)$ and $P(\theta)$ curves were normalized to a value of 1 at 10°. All measurements were conducted at room temperature [14, 15, 20–22].

2.3 Theoretical light scattering analysis

Philip Laven's software based on scattering (`MiePlot v4621`) was used to generate theoretical Volume scattering function and Degree of linear polarization plots for BT. Key input parameters included the refractive indices of the particles and the surrounding medium, the modal particle radius, the angular resolution, and the incident wavelength. These values were manually input into the software, which calculates the angular scattering behavior based on Mie theory [12, 17]. While effective for idealized spherical particles, the software does not account for temperature effects or irregular particle shapes, limiting its ability to fully replicate the complexities observed in experimental BT data. Table 1 outlines the vital inputs of BT employed in the theoretical calculations for data analysis. Fig. 2 and Fig. 3 present a comparison between the Mie plot and the experimental results for BT, highlighting differences in the angular distribution of $\beta(\theta)$ and $P(\theta)$.

Table 1: Parameters used in the theoretical analysis of BT particles.

Parameter	Value
Modal radius	0.250 μm
Refractive index	1.42
Wavelength	632.8 nm
Angular resolution	1°

3 Results and Discussion

3.1 Observed $\beta(\theta)$ for Black Turmeric

The graph compares $\beta(\theta)$ corresponds to BT using experimental data (blue line) with a theoretical Mie scattering model (red line) at a wavelength of 632.8 nm at room temperature. Table 2 below compares the experimental volume scattering function of BT and the theoretical predictions based on Mie scattering. Key characteristics such as peak location, sharpness, tail behavior, and symmetry are evaluated to highlight the differences between practical observations and idealized modeling. The graph in Fig. 3 illustrates how the scattering behavior of BT particles diverges from theoretical expectations derived from Mie theory. Although both the experimental and Mie curves peak near 90°, the BT data reveals more abrupt and uneven variations around this angle. Mie theory, which

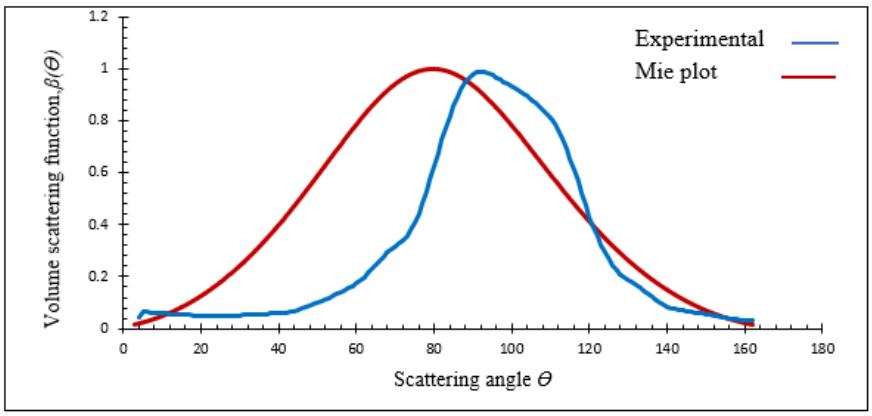

Figure 3: Comparison of measured $\beta(\theta)$ for BT: Experimental vs. Mie plot

assumes uniform, spherical particles, predicts a smooth and gradual scattering profile, but the BT plot exhibits a sharper maximum and steeper intensity drop-off on either side. These sharper features in the BT profile point to more complex interactions, likely caused by the irregular morphology of BT. Notably, the rapid decrease in scattering intensity beyond 90° in the BT curve contrasts with the gentler decline suggested by the Mie model. This discrepancy can be attributed to factors such as surface morphology, size distribution in the sample, and the porous or ”fluffy” texture of the BT sample, all of which influence light scattering in ways that simplified models cannot replicate. Furthermore, Mie theory computations typically involve a single particle radius that is modal radius, whereas real-world experiments involve a diverse mix of particle sizes and shapes. This difference contributes to the observed mismatch between theory and experiment. Consequently, the BT curve underscores the inherent limitations of applying Mie theory to organic systems, which often defy the assumptions of homogeneity and uniformity.

3.2 Observed $P(\theta)$ for Black Turmeric

The graph illustrates a comparison between the experimentally measured $P(\theta)$ of BT (blue line) and the corresponding theoretical prediction derived from Mie scattering theory (red line). Both datasets correspond to a wavelength of 632.8 nm under room temperature conditions. Complementing the visual comparison, Table 2 presents a side-by-side evaluation of key features of the experimental and theoretical $P(\theta)$, including peak position, sharpness, symmetry, and tail characteristics. This comparison sheds light on the discrepancies between real-world behavior and the idealized Mie model.

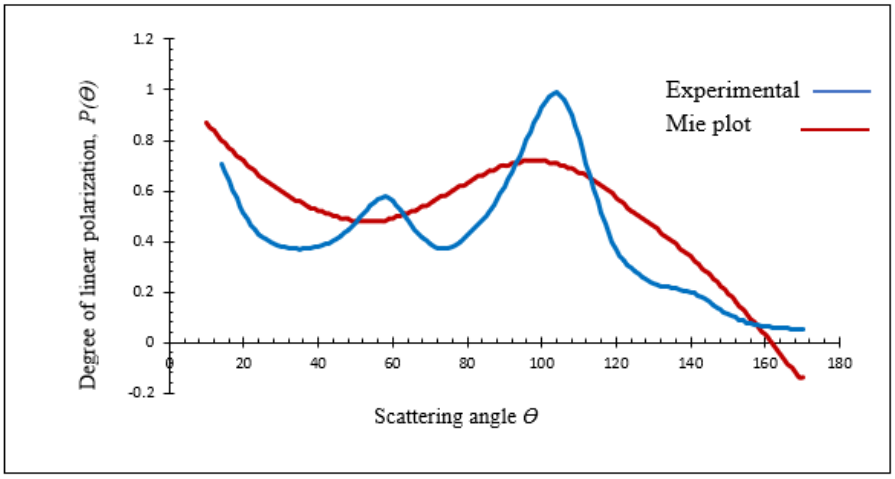

Figure 4: Comparison of Measured $P(\theta)$ for BT: Experimental vs. Mie plot

Feature	Experimental	Theoretical (Mie Plot)
Peak Location	Prominent peak around 60°	Peak occurs gradually near 90°
Sharpness	Sharp and well-defined peaks with local fluctuations	Smooth and broad peak with gradual transitions
Tail Behavior	Steep decline beyond 120°, even turning negative (polarization reversal)	Gradual descent with values staying positive throughout
Profile distribution	Asymmetric with multiple irregular features	Fairly symmetric around the peak, typical of ideal spherical scattering

Table 2: Comparison of $P(\theta)$ Characteristics: Experimental vs. Theoretical

The graph in Fig. 4 compares the $P(\theta)$ of BT using experimental data and theoretical predictions based on Mie scattering. The experimental curve (blue line) shows a non-linear variation of $P(\theta)$ with a scattering angle, characterized by multiple peaks. A prominent peak appears around 60°–70°, followed by a dip and a smaller peak near 110°, after which the $P(\theta)$ gradually decreases and exhibits slight fluctuations beyond 120°. This curve is asymmetric and irregular, reflecting the complexities that might have arisen due to temperature, size distribution, shape distribution, etc. [14, 15]. In contrast, the theoretical Mie plot (red line) exhibits a smooth and symmetrical profile, peaking broadly near 90° and gradually decreasing on either side of the angle range. Unlike the experimental data, it lacks sharp features or oscillations. These deviations arise because:

1. Inclusion of a single size parameter that is modal radius in the `MiePlot` software.
2. Size dependence of polarization and depolarization effects.
3. Possible alignment or organic particles due to gravity settling.

The $\beta(\theta)$ and $P(\theta)$ results emphasize the limitations of applying classical scattering models like Mie theory to biologically derived or structurally complex materials. These findings highlight the necessity for more advanced and flexible modeling tools that can account for real-world factors such as particle size and shape distributions. Notably, all experiments were performed at room temperature; however, the Mie plotting software used for theoretical predictions lacks the ability to incorporate temperature as a variable. Since temperature can influence the morphological characteristics of the particles in a medium, its exclusion may contribute to discrepancies between theoretical and experimental results. Therefore, integrating size and size distribution, shape and shape distribution, temperature control, or adjustment features into Mie modeling software would enhance its accuracy and relevance for experimental comparisons. Furthermore, environmental influences and measurement uncertainties, such as detector sensitivity, alignment errors, and ambient light, can also play a role in the observed deviations. This enables a relative assessment of the reported scattering matrix elements of BT from experimental measurements and theoretical predictions.

4 Conclusion

This study demonstrates the limitations of classical Mie theory in accurately modeling the light scattering behavior of randomly oriented sub-micron BT particles. Experimental measurements of the scattering matrix elements d_{11} and d_{12}, obtained using a He-Ne laser at 632.8 nm, revealed notable deviations from theoretical predictions. These discrepancies are primarily attributed to the complex particle size, shape, and distribution inherent in the BT samples, factors not accounted for in the idealized assumptions of Mie theory. While experimental investigations can be extended to varying temperature conditions, current theoretical models lack the flexibility to incorporate such variations. Overall, the comparative analysis offers valuable insights into the optical properties of BT and underscores the need for more advanced scattering models to better represent biologically complex materials. The experimental database can be created for different sizes, size distributions, temperatures, etc which will serve as a tool for better classification.

Acknowledgement

The authors wish to thank Dr. Ratan Boruah, Sophisticated Analytical Instrumentation Centre (SAIC), Tezpur University, Assam, India for his help in characterizing the Black turmeric, by SEM analysis technique.

Author contributions

SR conceived the study, FH and SR performed research, generated the scattering profiles, and analyzed figures and data. FH wrote the main manuscript, and SR and FH reviewed the results and the main manuscript.

Data Availability Statement

All data generated or analyzed during this study are included in this article.

Declarations

Conflict of interest: The authors declare no competing interests.

References

[1] A. R. Jones, Progress in Energy and Combustion Science **25**, 1 (1999).

[2] H. Zhao, X. Wang, R. Wang, D. Hua, K. Li, and F. Ji, Measurement Science and Technology **34**, 125802 (2023).

[3] E. Huber and M. Frost, Journal of Water Supply: Research and Technology–Aqua **47**, 87 (1998).

[4] L. A. Clementi, J. R. Vega, L. M. Gugliotta, and A. Quirantes, Journal of Quantitative Spectroscopy and Radiative Transfer **113**, 2255 (2012).

[5] H. E. Redmond, K. D. Dial, and J. E. Thompson, Aeolian Research **2**, 5 (2010).

[6] J. Flammer, M. Mozaffarieh, and H. Bebie, *Basic sciences in Ophthalmology: Physics and Chemistry* (Springer, 2013).

[7] M. I. Mishchenko, J. W. Hovenier, and L. D. Travis, eds., *Light Scattering by Nonspherical Particles: Theory, Measurements, and Applications* (Academic Press, San Diego, 2000).

[8] M. I. Mishchenko, Journal of Quantitative Spectroscopy and Radiative Transfer **110**, 1210 (2009).

[9] S. Yushanov, J. S. Crompton, and K. C. Koppenhoefer, in *Proceedings of the COMSOL Conference*, Vol. 116 (Cosmol Inc. Boston, 2013) pp. 1–7.

[10] W. Hergert and T. Wessels, eds., *The Mie Theory: Basics and Applications*, Springer Series in Optical Sciences, Vol. 169 (Springer-Verlag, Berlin, Heidelberg, 2012).

[11] M. J. Cheng, Y. C. Cao, K. F. Ren, H. Zhang, and L. X. Guo, Frontiers in Physics **12**, 1 (2024).

[12] F. Hussain, J. Hussain, S. S. Khanam, S. Noorani, A. B. Bhattacherjee, and S. Roy, Scattering phase functions and polarimetric responses of selected bioparticles, in *Optical Polarimetric Modalities for Biomedical Research*, edited by N. Mazumder, Y. V. Kistenev, E. Borisova, and S. Prasada K. (Springer International Publishing, Cham, 2023).

[13] P. Laven, Applied Optics **44**, 5667 (2005).

[14] F. Hussain, H. P. Jaishi, and S. Roy, Journal of Physics: Conference Series **2919**, 012046 (2024).

[15] F. Hussain, H. P. Jaishi, and S. Roy, in *Emerging Trends in Physical Science*, edited by B. Choudhury, D. P. Mahanta, and S. K. Sharma (Anundoram Borooah Academic Society, Assam, India, 2024).

[16] J. M. Steinke and A. P. Shepherd, Appl. Opt. **27**, 4027 (1988).

[17] F. Hussain, N. Mazumder, and S. Roy, Lasers in Medical Science **38**, 107 (2023).

[18] V. J. Dennis, Just Agriculture **2**, 1 (2021), e-ISSN: 2582-8223.

[19] A. Venugopal, K. A. Rinu, and D. Joseph, Innoriginal International Journal of Sciences **4**, 1 (2017).

[20] F. Hussain and S. Roy, The European Physical Journal Plus **139**, 687 (2024).

[21] S. Roy, F. Hussain, and N. Mazumder, Discover Applied Sciences **7**, 235 (2025).

[22] S. Roy, R. Mahatta, N. Barua, A. K. Buragohain, and G. A. Ahmed, Journal of Quantitative Spectroscopy and Radiative Transfer **112**, 1784 (2011).